A lattice Boltzmann study on trade-off between mixing and flow efficiency for electroosmotic flow in heterogeneous microchannels with nonuniform surface potentials

Fuzhi Tian, Daniel Y. Kwok*

Nanoscale Technology and Engineering Laboratory, Department of Mechanical Engineering, University of Alberta, Edmonton, Alberta T6G 2G8, Canada

Abstract

A lattice Boltzmann model (LBM) is used to simulate electroosmotic flow (EOF) in a rectangular microchannel with nonuniform surface potentials. The simulation results indicate that local circulations can occur near a heterogeneous region. The largest circulations, which imply the highest mixing efficiency due to convection and short-range diffusion, were found when the average surface potentials is zero. More importantly, we have illustrated that there is a trade-off between the mixing and flow efficiency in EOF microfluidics.

Keywords: LBM; Electroosmotic flow; Nonuniform surface potential; Mixing

1. Introduction

Both fluid transport and mixing with high efficiency are required simultaneously in microchannel network devices for chemistry and biochemistry. To achieve a sufficient mixing can be a challenge due to low Reynolds number. Recently, many studies have shown that electroosmotic flow (EOF) with nonuniform surface electric potential can enhance mixing due to the electrical double layer (EDL) effect [1,2,3,4,5]. We note, however, that there is a trade-off between such mixing and flow efficiency, and this important factor has often been ignored. Therefore, the purpose of this study is to investigate this trade-off for electroosmotic flow in heterogeneous microchannels by means of a lattice Boltzmann model (LBM) [6,7,8,9,10,11].

2. LBM method and EDL theory

We employ a D2Q9 LBM scheme proposed in [8] to simulate the flow field. For EOF driven by an external electric field E_{ext}, the external force term F can be expressed as $F = \rho_e E_{ext}$, where ρ_e is the net charge density in the EDL, obtained by solving the Poisson-Boltzmann equation [12].

3. Results and discussion

In Fig. 1, the microchannel has a height of 0.5 μm and ψ_n and ψ_p are defined as the surface potentials for the negatively and positively charged patches with the lengths of L_n and L_p, respectively. The average surface potential ψ_{avg} of the channel can be calculated from

$$\psi_{avg} = \frac{\psi_p L_p + \psi_n L_n}{L_p + L_n} \tag{1}$$

In our simulation, a symmetric 1:1 electrolyte solution with an ionic molar concentration of 0.1 mM, having an EDL thickness of 30.4 nm, is selected. The externally applied electric field was set to be 1000 V/m.

3.1. Influence of the nonuniform surface potential on the flow field

Symmetric with $L_n/L_p = 1$ and $L_n/L_p = 4$: figs 2(a) and (b) shows two velocity fields for $L_n/L_p = 1$. As expected, the flow fields presented in these figures exhibit local circulations near the heterogeneous region. Smaller

* Corresponding author. Tel.: +1 (780) 492 2791; Fax: +1 (780) 492 2200; E-mail: daniel.y.kwok@ualberta.ca

Computational Fluid and Solid Mechanics 2005
K.J. Bathe (Editor)

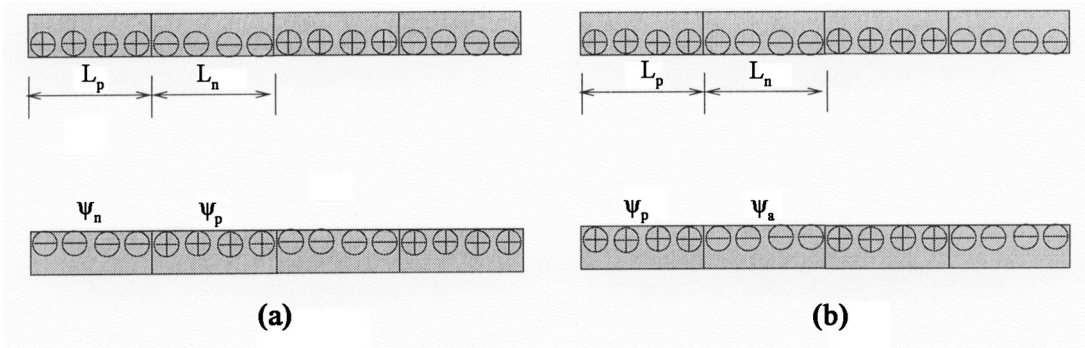

Fig. 1. Schematic of the patterned surfaces with (a) a symmetric (b) asymmetric stepwise variation of surface potential. ψ and L are the surface potential and length of the patches, respectively. The subscripts n and p represent the negatively and positively charged surfaces, respectively.

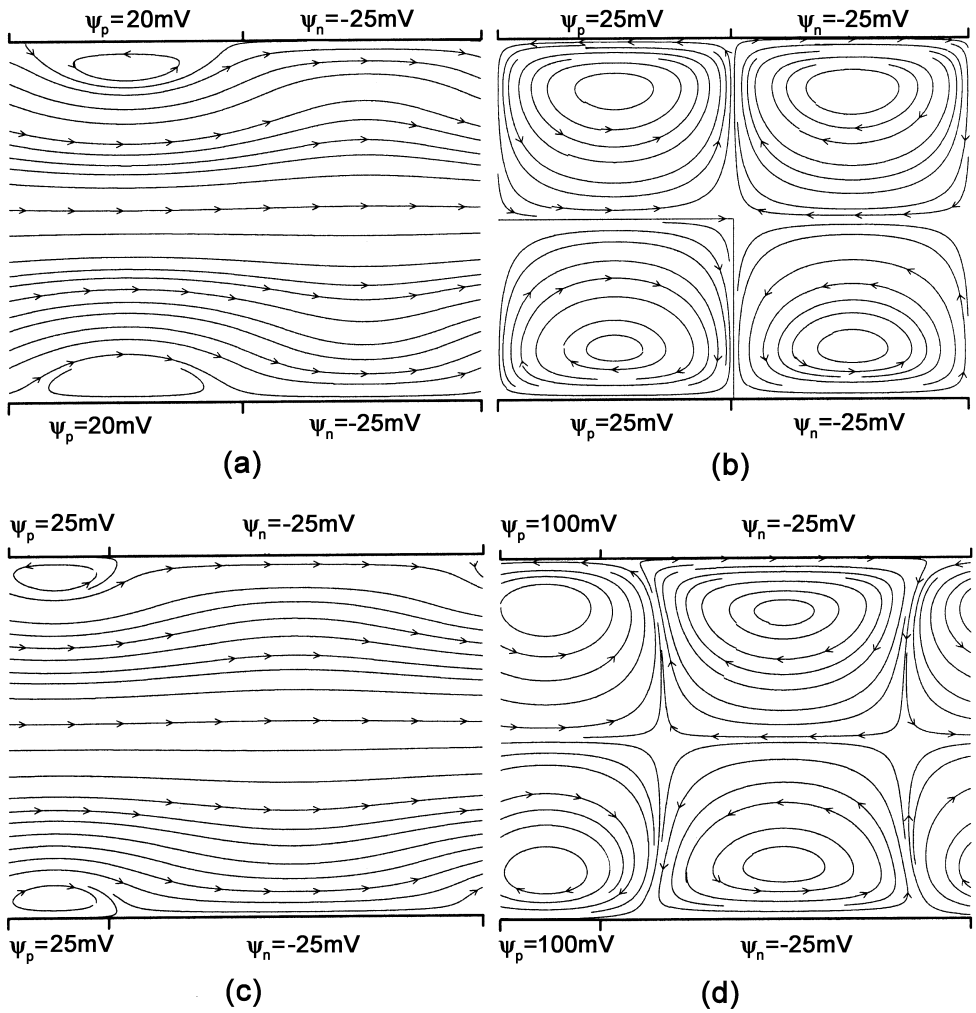

Fig. 2. Flow fields for a symmetrically arranged nonuniform surface potential when $\psi_n = -25\,\mathrm{mV}$ and (a) $\psi_p = 20\,\mathrm{mV}$ and $L_n/L_p = 1$; (b) $\psi_p = 25\,\mathrm{mV}$ and $L_n/L_p = 1$; (c) $\psi_p = 25\,\mathrm{mV}$ and $L_n/L_p = 4$; (d) $\psi_p = 100\,\mathrm{mV}$ and $L_n/L_p = 4$.

circulation was found in Fig. 2(a) when $\psi_p = 20$ mV. A larger circulation results from setting $\psi_p = |\psi_n|$ in Fig. 2(b) where the average surface potential ψ_{avg} is zero. Given the same surface potential as that in Fig. 2(a), if the ratio of L_n/L_p is set to be 4 in Fig. 2(c), the size of the vortex in Fig. 2(c) decreases due to the smaller patch size of L_p. If the surface potential ψ_p increases to 100 mV for $L_n/L_p = 4$, shown in Fig. 2(d), we obtain the biggest circulations with various sizes due to zero average surface potential. Thus, the patterns of the flow fields are dramatically different due to the magnitude and size of the positively charged heterogeneous regions.

Asymmetric with $L_n/L_p = 1$ and $L_n/L_p = 4$

The heterogeneous patches here are arranged asymmetrically. In Fig. 3(a)–(d), it is apparent that the vortex positions shift. Comparing the flow fields in Figs 2(b) and 3(b), we see that the direction of the vortex has changed as a result of rearrangement of the heterogeneous patches. For the ratio of $L_n/L_p = 4$, the flow field in Fig. 3(d) shows that the larger the dimension L_n is, the bigger the circulation size is. Because of the asymmetric distribution and dimension of the charged patches, the flow field in Fig. 3(d) is the most tortuous. Overall, these circulation regions force the bulk to flow through a narrower channel cross section, which enhances mixing because of shorter local diffusion and convection. In addition, we see by comparing Figs 2(b),

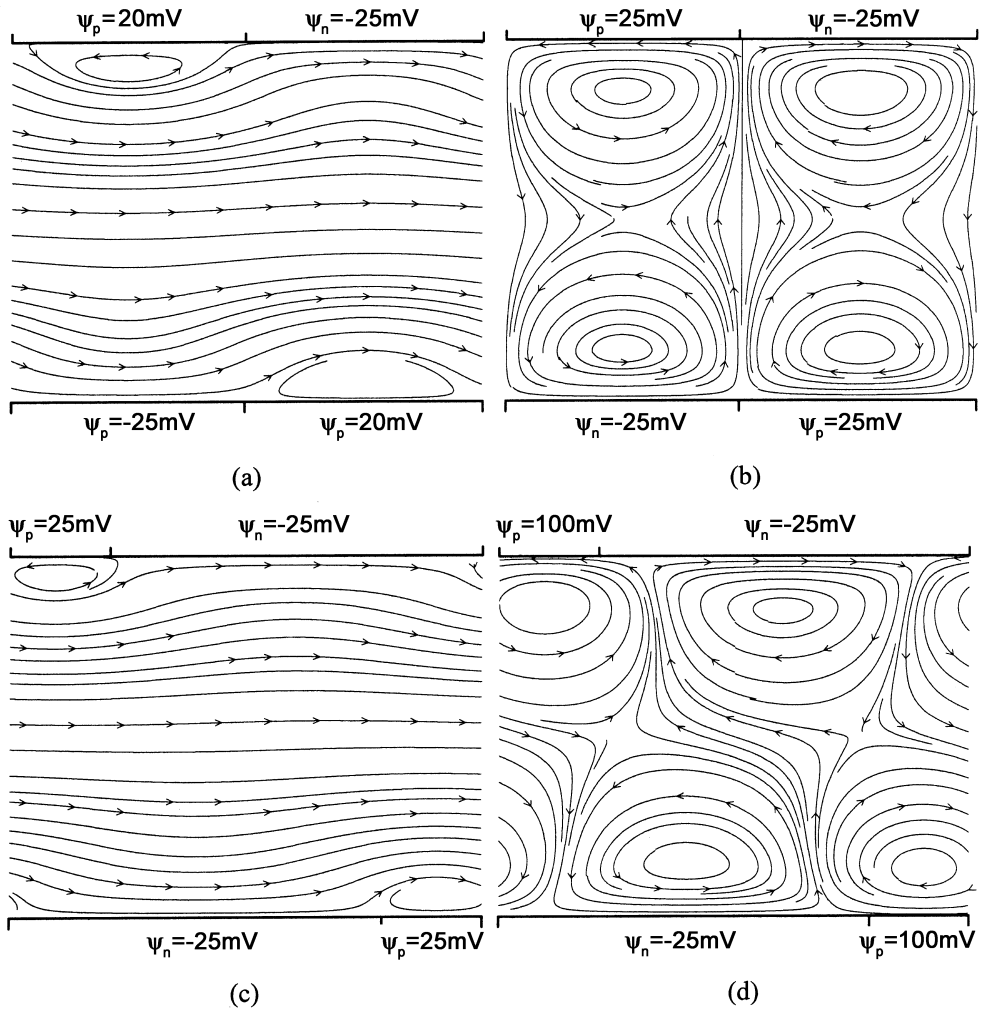

Fig. 3. Flow fields for an asymmetrically arranged nonuniform surface potential when $\psi_n = -25$ mV and (a) $\psi_p = 20$ mV and $L_n/L_p = 1$; (b) $\psi_p = 25$ mV and $L_n/L_p = 1$; (c) $\psi_p = 25$ mV and $L_n/L_p = 4$; (d) $\psi_p = 100$ mV and $L_n/L_p = 4$.

2(d), 3(b) and 3(d) that movement perpendicular to the applied field can be generated in the circulation regions. This type of motion could be particularly useful in mixing.

3.2. Influence of nonuniform surface potential on the volumetric flow rate

The volumetric flow rate Q is normalized by the maximum flow rate Q_{max} with uniform surface potential of $\psi = -25$ mV in the same channel. From Fig. 4, we see that Q/Q_{max} decreases linearly as ψ_p increases for both curves A and B and for the same surface potential ψ_p, Q/Q_{max} for $L_n/L_p = 1$ (curve B) is smaller than that when $L_n/L_p = 4$ (curve A). Figure 5 shows the dependence of Q/Q_{max} on the ratio $L_p/(L_n + L_p)$. It is again apparent that Q/Q_{max} decreases linearly as the ratio $L_p/(L_n + L_p)$ increases for both symmetric and asymmetric cases. It is then instructive to study how Q/Q_{max} changes with the average surface potentials ψ_{avg} defined in Eq. (1). From Fig. 6, we see that Q/Q_{max} indeed depends linearly only on the average surface potential ψ_{avg} even though the individual flow field could have been different. Therefore, we conclude that arrangement of nonuniform surface potential has no effect on the flow rate.

3.3. Trade-off between mixing and flow efficiency of microfluidics

According to results in Figs 2 and 3, we see that more complex patterns of the heterogeneous surface potential will enhance mixing to higher efficiency because of circulation and tortuosity. In order to obtain larger circulation and tortuosity, the average surface potential ψ_{avg} should be as close to zero as possible. However, from the flow rate discussion above in Fig. 6, as ψ_{avg} approaches zero, the normalized flow rate Q/Q_{max} also decreases to zero. Indeed, there is a trade-off between the mixing efficiency and flow efficiency via circulations induced by heterogeneous surface potential. Thus, design and applications of such phenomena for mixing should be carefully considered. On the one hand, mixing is required; on the other, liquid transport is also an important issue for electroosmotic flow.

4. Conclusions

A lattice Boltzmann method has been used to simulate electroosmotic flow in a 0.5 μm microchannel with heterogeneous surface potential. The simulation results indicate that local circulations can be obtained near the heterogeneous region, in agreement with those obtained

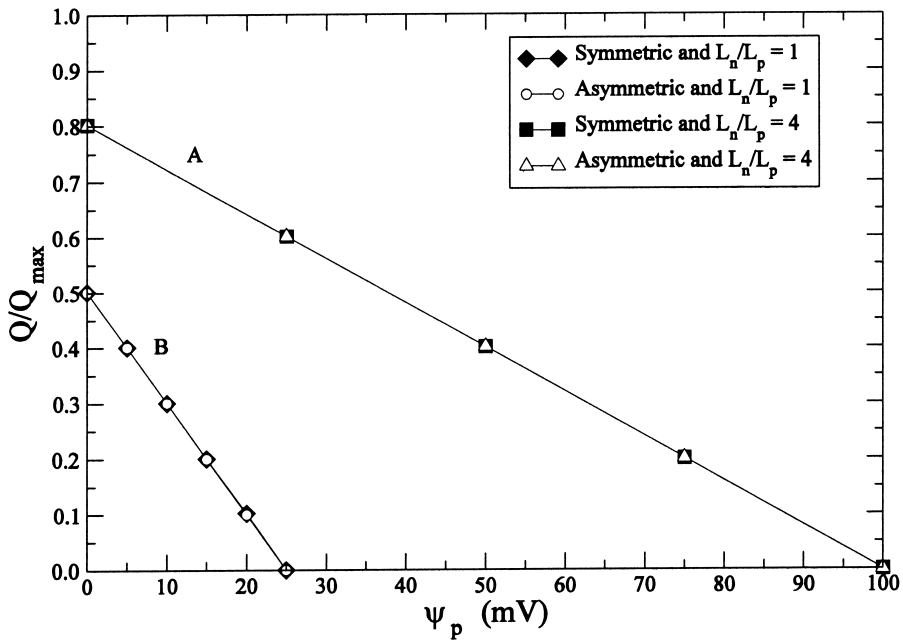

Fig. 4. Normalized volumetric flow rate versus surface potential of the positively charged region ψ_p when $\psi_n = -25$ mV. Curve A represents the case of $L_n/L_p = 4$ and $\psi_p = 0$, 25, 50, 75, and 100 mV; Curve B represents the case of $L_n/L_p = 1$ and $\psi_p = 0$, 5, 10, 15, 20, and 25 mV.

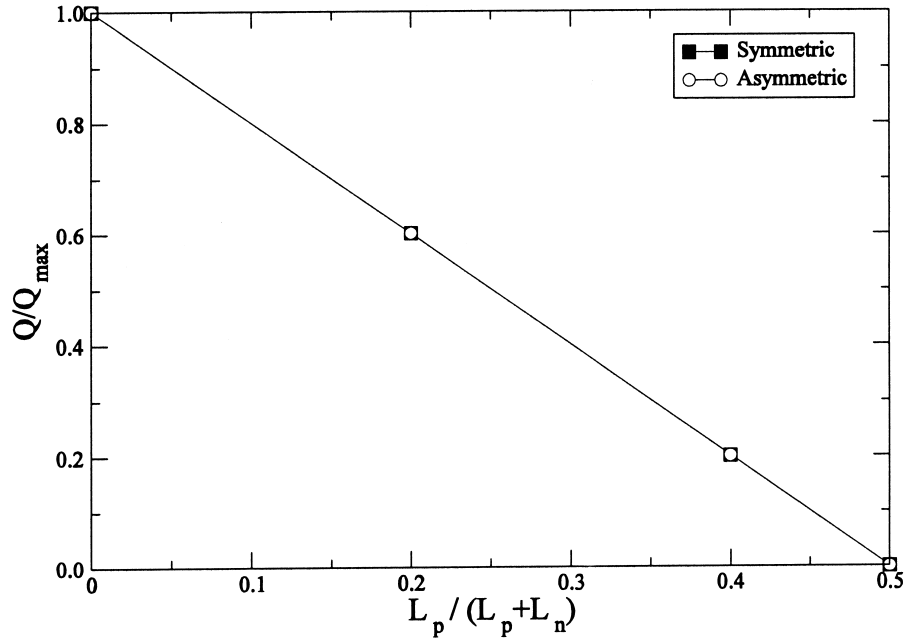

Fig. 5. Normalized volumetric flow rate versus length ratio of the positively charged region L_p ($L_p + L_n$) for $\psi_p = |\psi_n| = 25\,\text{mV}$.

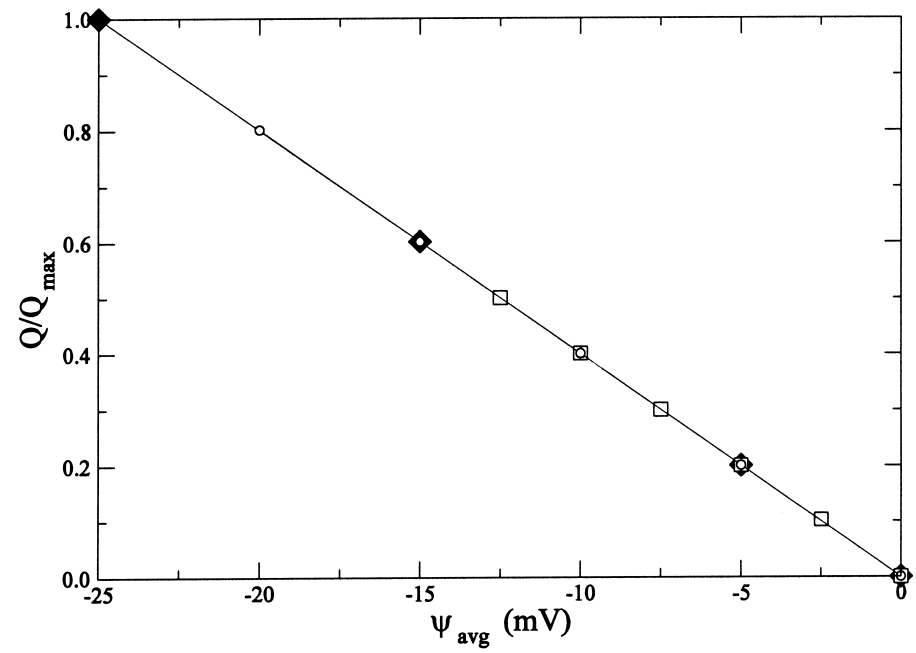

Fig. 6. Normalized volumetric flow rate versus average surface potential ψ_{avg} when $\psi_n = -25\,\text{mV}$ and □: $L_n/L_p = 1$ and $\psi_p = 0$, 5, 10, 15, 20, and 25 mV; ◆: $\psi_p = 25\,\text{mV}$ and $L_p/(L_p + L_n) = 0$, 0.2, 0.4, and 0.5; o: $L_n/L_p = 4$ and $\psi_p = 0$, 25, 50, 75, and 100 mV.

by other authors using the traditional CFD method. Different patterns of the heterogeneous surface potential cause different magnitude of the circulation. The largest circulation, which implies the highest mixing efficiency due to convection and short-range diffusion, was found when the average surface potential is zero. A zero average surface potential, however, implies zero flow rate. We have shown that there is a clear trade-off between the mixing efficiency and flow efficiency in microfluidics with heterogeneous surfaces.

Acknowledgment

We gratefully acknowledge financial support from the Canada Research Chair (CRC) Program and Natural Sciences and Engineering Research Council of Canada (NSERC) in support of this research.

References

[1] Patankar NA, Hu HH. Numerical simulation of electro-osmotic flow. Analytical Chem 1998;70:1870–1881.
[2] Yang RJ, Fu LM, Lin YC. Electroosmotic flow in microchannels. J Colloid Interface Sci 2001;239:98–105.
[3] Ajdari A. Electroosmosis on inhomogeneously charged surface. Phys Rev Lett 1995;75:755–758.
[4] Stroock AD, Weck M, Chiu DT, Huck WT, Kenis PJA, Ismagilov RF, Whitesides GM. Chaotic mixer for microchannels. Phys Rev Lett 2000;84:3314–3317.
[5] Erickson D, Li D. Influence of surface heterogeneity on electrokinetically driven microfluidic mixing. Langmuir 2002;18:1883–1892.
[6] Chen S, Doolen GD. Lattice Boltzmann method for fluid flow. Ann Rev Fluid Mech 1998;30:329–364.
[7] Luo LS. Theory of the lattice Boltzmann method: lattice Boltzmann models for nonideal gases. Phys Rev E 2002;62:4982–4996.
[8] Li B, Kwok DY. Discrete Boltzmann equation for microfluidics. Phys Rev Lett 2003;90:124502–1–4.
[9] Succi S. The Lattice Boltzmann Equation for Fluid Dynamics and Beyond. Oxford: Clarendon Press, 2001.
[10] Succi S, Benzi R, Higuera F. The lattice Boltzmann equation. A new tool for computational fluid dynamics. Physica D 1991;47(1):219–230.
[11] Melchionna S, Succi S. Electrorheology in nanopores via lattice Boltzmann simulation. J Chem Phys 2004;120:4492.
[12] Masliyah JH. Electrokinetic Transport Phenomena. OSTRA technical publication series, no. 12, Edmonton, AL: Alberta Oil Sands Technology Research Authority, 1994.